RELATION OF VISCOSITY CHARACTERISTICS IN CWM TO COAL RANK

JUNYA NISHINO, KAZUHIKO KIYAMA AND MASAO SEKI

Ishikawajima Harima Heavy Industries Co., Ltd., Research Institute, Chemical Process Technology Department, Yokohama 235

Key Words: Energy, Coal Water Mixtures, Coal Rank, Viscosity Characterization, Surface Chemistry

To establish an evaluation system of coals for CWM, attempts were made with twenty kinds of coal from various countries and locations to study the relations of the rank of coal as bulk material to viscosity characteristics in CWM, in addition to surface-chemical properties such as water vapor adsorption and zeta potential.

Various parameters of viscosity described in Fig. 2-b, such as ϕ_0, α and ϕ_{1000}, show almost the same tendency of reaching a constant level above about 85% carbon content in coal (Fig. 12 Curve a)—an outstanding feature of viscosity characteristics.

The same tendencies were also observed in zeta potential, quantities of adsorption of water on coal surface, ϕ_{AD}, and of water occluded within aggregates of coal particles, ϕ_{OC}.

The results on various parameters are rather scattered, and it is presumed necessary to study coal not only as bulk material but also on the basis of surface chemistry.

1. Introduction

Studies of coal–water mixtures (CWM) have been made in large numbers since about 1975, resulting in remarkable progress, particularly in practical technology.

However, attention to viscosity or stability of CWM in the field of basic research seems to have been paid rather to coals as bulk material. Investigation is still necessary to establish an evaluation system of coals for CWM technology from the standpoint of the surface chemistry of coal particles, especially of functional groups distributed on the coal surface in addition to surface physical properties, such as particle size, surface tension and zeta potential.

Progress in analytical methods for oxygen containing functional groups has been marked since about 1965,[1,5,9,12] promoting investigations of surface chemical and physical properties such as wettability,[4] water adsorption,[1,3,4,6,8,9,13] viscosity[7,11] and functional groups of lower-rank coals.[10]

However, these investigations seem to remain confined to vague indications of the relation between functional groups and various properties of CWM. As the first step in establishing an evaluation system of coals for CWM, attempts were made to study the relation of rank of coal as bulk material to viscosity characteristics in CWM, in addition to surface-chemical properties such as water vapor adsorption and zeta potential.

Received January 18, 1988. Correspondence concerning this article should be addressed to J. Nishino. Superconductivity Research Laboratory, 1-10-13 Shinonome, Koto-ku, Tokyo 135, Japan.

2. Samples and Experiments

In **Table 1** are included twenty coals from various locations for testing, which give the well-known relation between carbon content and oxygen content in coals shown in **Fig. 1**. Since anomalies can hardly be seen, the selection is considered to be appropriate. In addition, soda lime-glass powder was used for comparison.

Coals were put into a ball mill made of alumina with non-ion distilled water, followed by crushing with stainless steel balls until coal particles of size under 74 μm increased to above 70 wt%. According to a Rosin-Rammlar plot, the exponent of size distribution (particle size of 1–300 μm) was 0.9–1.2 and mean particle size was 30–40 μm. Rheological properties of slurries are generally affected by mean particle size, maximum particle size and size distribution. However, since the main purpose of this report is to establish the relation between viscosity characteristics of CWM and coal rank, pretreatment conditions were not changed in this study. After such preparation, all measurements were made within 5 h.

Addition of formalin-condensed sodium salt naphthalene sulfonic acid as dispersant was 0.5 wt% on dry basis to coal, unless otherwise stated.

Measurement of viscosity was made by a rotary viscometer of double-drum type placed in a thermostated bath at 293 K. Shear rate applied to CWM was increased from zero to 114 s^{-1} in 2.5 min, kept at this level for 2 min, and then decreased. This was the first cycle, and during the decreasing stage of the second cycle the apparent viscosity was obtained by

Table 1. Analysis of coals and flow type of CWM tested

No. of coal	Coal name	Country[1]	Approximate analysis [wt%]				Ultimate analysis [wt%]					Flow type of CWM at 1000 mPa·s[2]	(Volume fraction of coal ϕ_{1000})
			F.C.	V.M.	Ash	I.M.	C	H	O	N	S		
1	TH	JPN	35.5	41.7	16.2	6.6	76.0	6.4	16.2	1.2	0.2	O_s	(0.540)
2	MR	AUS	57.2	29.8	9.0	4.0	82.1	5.2	10.3	2.0	0.4	P-II	(0.560)
3	PC	USA	52.5	34.5	9.0	4.0	78.6	5.7	13.8	1.5	0.4	P-I	(0.595)
4	CZ	AUS	57.9	25.3	14.8	2.0	84.1	5.0	8.6	1.8	0.5	P-I	(0.600)
5	BL	CAN	69.6	19.3	10.0	1.1	88.5	4.9	5.1	1.2	0.3	P-I	(0.632)
6	SG	JPN	29.8	29.2	37.8	3.2	78.1	6.0	12.2	2.1	1.6	O_s	(0.562)
7	HR	JPN	37.2	40.4	18.9	3.5	80.6	6.8	10.7	1.5	0.4	P-II	(0.567)
8	TT	CHI	58.8	28.7	6.6	5.9	83.0	4.9	10.3	0.9	0.9	O_s	(0.536)
9	CV	CAN	44.2	31.9	11.2	12.7	77.4	4.9	16.3	1.1	0.3	O_s	(0.477)
10	CB	CAN	62.4	33.7	2.6	1.3	86.2	5.6	5.4	1.7	1.1	P-I	(0.611)
11	SV	AUS	52.0	30.3	14.2	3.5	84.2	5.4	8.1	1.8	0.5	P-II	(0.575)
12	WW	AUS	52.4	30.2	14.3	3.1	83.1	5.4	9.0	1.9	0.6	P-II	(0.608)
13	UL	AUS	52.1	31.7	12.4	3.8	84.7	5.1	7.8	1.8	0.6	P-I	(0.610)
14	BA	AUS	52.3	28.3	11.3	8.1	81.6	5.1	10.9	1.7	0.7	P-II	(0.522)
15	BL	THI	34.3	34.2	10.9	20.6	69.5	4.8	22.2	2.8	0.7	O_s	(0.324)
16	PL	USA	46.4	39.4	8.2	6.0	79.2	5.9	12.7	1.6	0.6	P-I	(0.574)
17	MT	AUS	49.1	29.3	18.5	3.1	82.6	5.4	9.5	2.0	0.5	P-II	(0.588)
18	JB	JPN	27.3	29.7	30.3	12.7	70.5	5.8	22.1	1.1	0.5	O_s	(0.504)
19	HG	VIE	85.6	6.7	5.2	2.5	92.6	3.5	2.4	1.1	0.4	P-I	(0.600)
20	RS	RSA	56.0	25.7	14.5	3.8	84.3	4.3	8.6	1.9	0.9	P-II	(0.622)

[1] JPN, Japan; AUS, Australia; USA, United States of America; CAN, Canada; CHI, China; VIE, Vietnam; RSA, South Africa.
[2] P-I, Initially pseudo-plastic flow followed by dilatant flow. P-II, Initially Ostwald flow followed by dilatant flow. O_s, Initially Ostwald flow followed by Bingham flow.

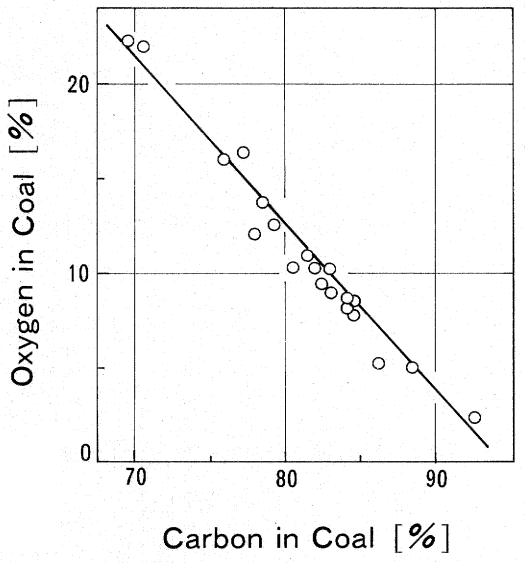

Fig. 1. Relation between oxygen and carbon in coals tested

measuring shear stress at $100\,s^{-1}$.

Measurement of size distribution of coal particles was made by the laser diffraction method, and of zeta potential by the electrophoresis method in 0.01 mol/l solution of potassium chloride.

Adsorption and swelling by water were measured using coals of 44–47 μm size after drying at 343 K and then keeping for 2 weeks in a desiccator containing NaCl-saturated aqueous solution at the bottom. Swelling was measured by the helium substitution method.

3. Results and Discussion

3.1 CWM flow type and kind of coal

There were essentially two types in flow of CWM, as shown in **Fig. 2-a**: pseudo-plastic flow at the stage of increasing stress in the first cycle, followed by dilatant flow at those of decreasing stress in the first and after the second (P-I type); and Ostwald flow followed by Bingham (Os type) flow. In addition, flow of a type intermediate between these two (P-II type) was observed.

As shown in Table 1, flow was of P-I type for seven kinds of coal, Os for six kinds and P-II for seven kinds.

3.2 Viscosity and coal concentration in CWM

The logarithmic relation of viscosity to volume fraction of coal (ϕ) in CWM is schematically revealed in **Fig. 2-b**, in which it is likely that log η has a linear relation with ϕ in higher ranges for practical use (region II).

ϕ_0 is introduced by interpolating this linear line to the level of viscosity of water as a solvent, being probably regarded as the lowest volume fraction to induce mutual interaction between particles in disregard of the presence of region I. α is the slope of this linear line. Additionally, region III is probably a range in which a group of particles separates from CWM.

ϕ_R, ϕ_I and [B] in Fig. 2-b will be defined in relation

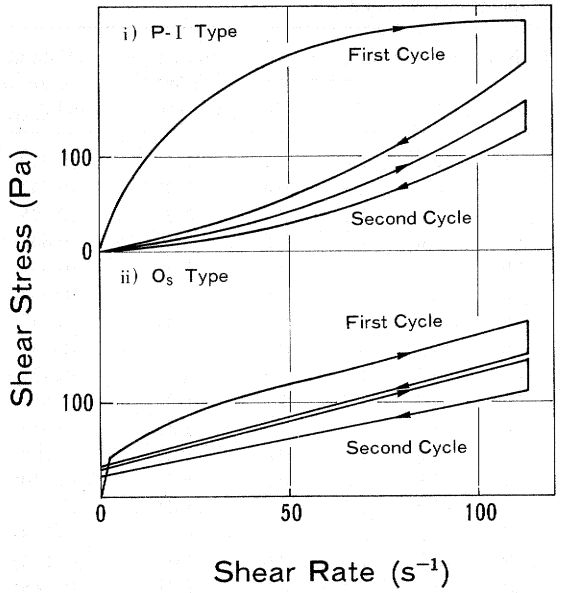

Fig. 2-a. Schematic representation of flow type

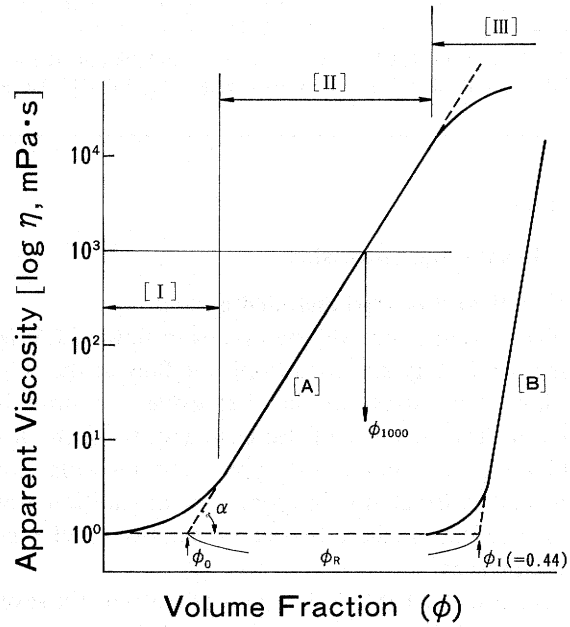

Fig. 2-b. Schematic representation of relation between concentration of powder and apparent viscosity in slurries
Powder
[A] Coal
[B] Material without adsorption and coagulation

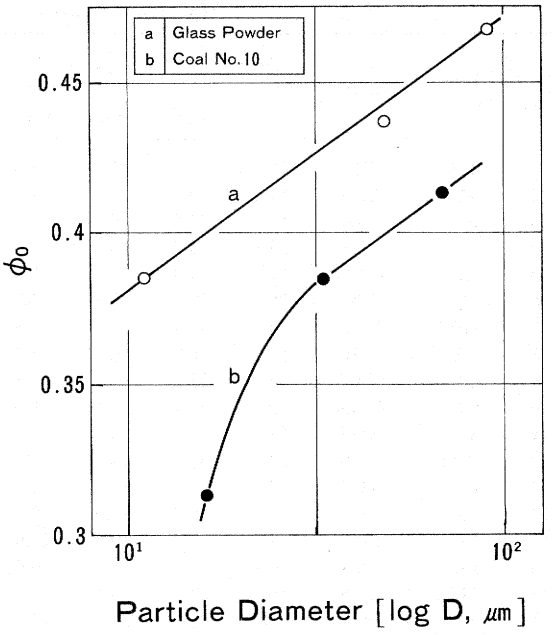

Fig. 3. Effect of particle size on ϕ_0

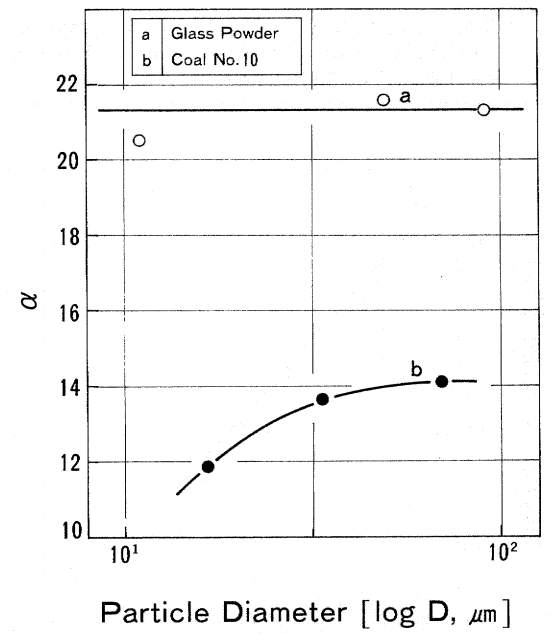

Fig. 4. Effect of particle size on α

to Fig. 9 in the next section.

Figures 3 and **4** reveal the dependences of particle size on ϕ_0 and α, respectively, showing that the larger the particle size, the greater the ϕ_0. In the case of glass it may be noticeable that the dependences are less marked and α is very high.

The relations of ϕ_0 and α to carbon content in coal are shown in **Fig. 5**, in which it is clear that both ϕ_0 and α reach a constant level above about 85% carbon content (C_0). The relation of ϕ_{1000} at apparent viscosity of 1000 mPa·s (Fig. 2-b) to carbon content shows a similar trend.

Viscosity characteristics in higher-rank coals and glass behave in a similar manner. It is highly probable that this behavior originates in the weakness of mutual interaction other than friction between particles, in other words, in the difficulty of coagulation of particles.

As shown in Fig. 5, CWM of lower-rank coals exhibits Os type flow, while higher-rank coals exhibits P-I type flow and coals in the intermediate range (78–85% carbon content) exhibit P-II type flow.

As the addition of dispersant to CWM increases, zeta potential decreases and reaches a minimum. The

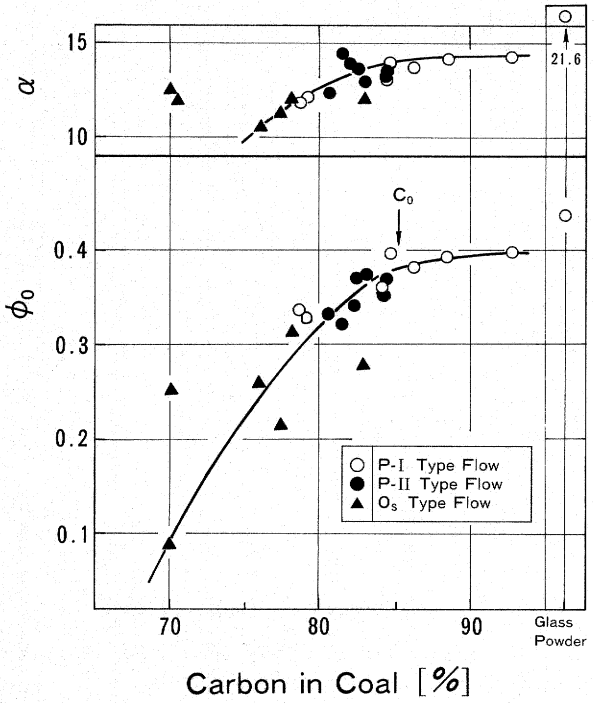

Fig. 5. Relation of ϕ_0 and α with carbon content in coal

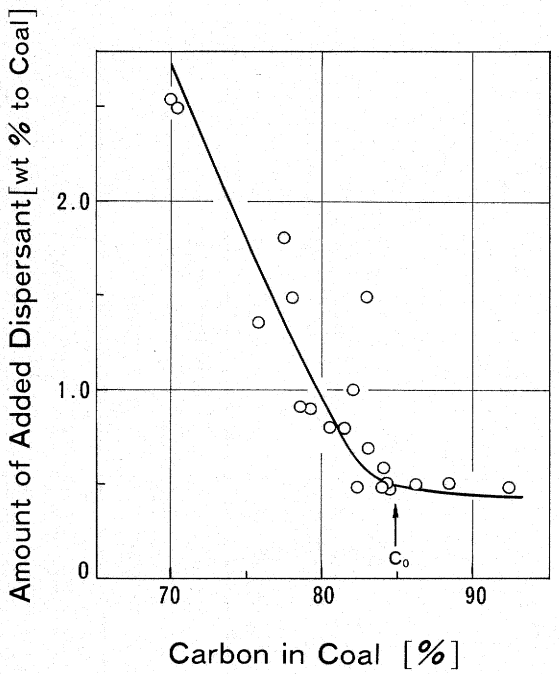

Fig. 6. Relation of amount of dispersant added for minimizing zeta potential with carbon content in coal

relation between the amount of dispersant at minimum zeta potential and carbon content of coal is shown in **Fig. 6**. Although the results are rather scattered, it may be said that it reaches a constant level above about 85% carbon content (C_0).

3.3 Water adsorption and viscosity characteristics

Since water adsorption has an unfavorable effect on the fluidity of CWM because of the consumption of free water contributing to flow, it may be impossible

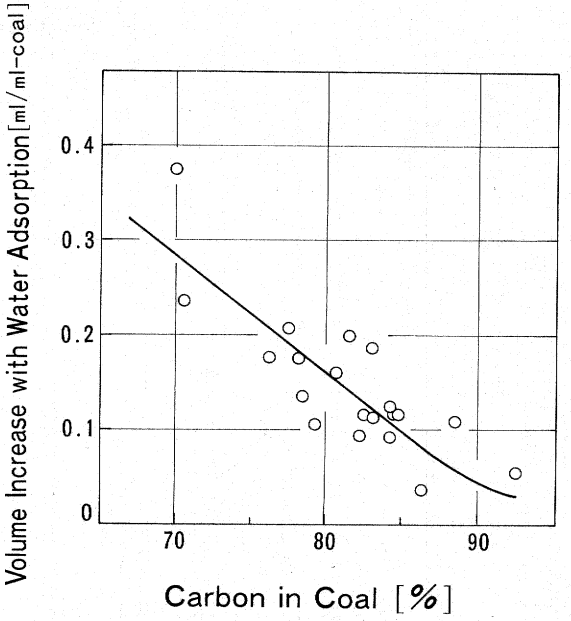

Fig. 7. Swelling with water adsorption versus carbon content in coal

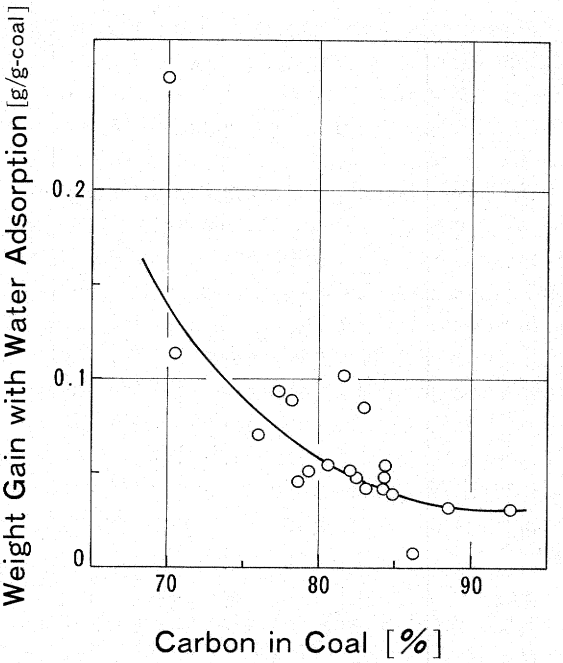

Fig. 8. Weight gain with water adsorption versus carbon content in coal

to disregard. The results of adsorption are shown by volume increase in **Fig. 7** and by weight increase in **Fig. 8**. Although the results are rather scattered, it may be said that the increase in volume is appreciably marked compared with weight increase.

According to Brenner,[2] the volume increase is mainly due to fine cracks mechanically generated in the inner layer rather than to physical or chemical change. Thus it may be relevant to mention that the increase in weight represents rather exactly the quantity of adsorption. Hereunder, volume increase by

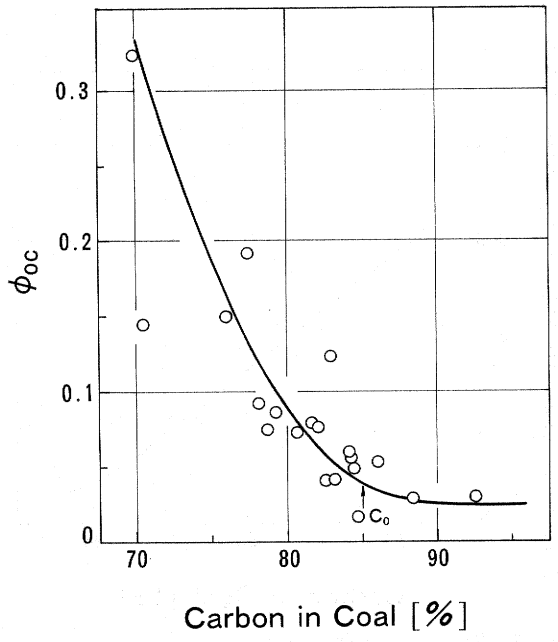

Fig. 9. Relation between carbon content in coal and ϕ_{OC}

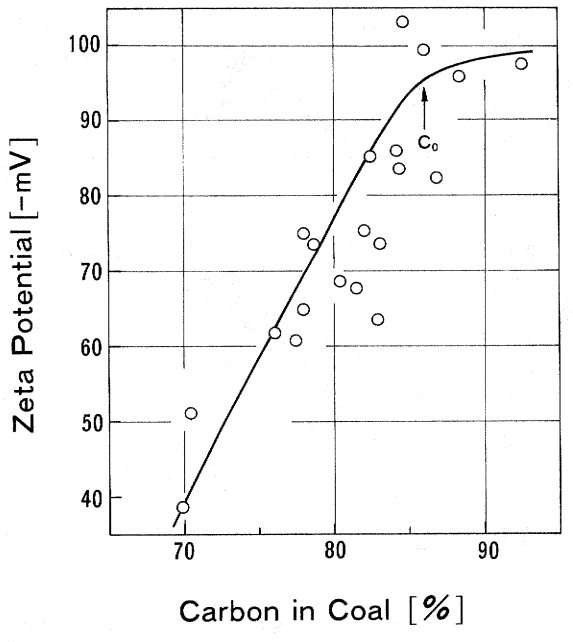

Fig. 10. Relation between carbon content in coal and zeta potential (Dispersant added in CWM: 0.5 wt%)

water adsorption is estimated from Fig. 8 on the assumption that the volume-to-weight ratio is approximately equal to unity.

There are two kinds of water in CWM other than chemically bound water, that is, (a) restricted water ϕ_R, (b) free water $1-\phi_I$, as shown schematically in Fig. 2-b. Here, ϕ_R seems to correspond to sum of adsorbed water ϕ_{AD} and water physically occluded within aggregates of particles ϕ_{OC}. To the volume fraction of coal in CWM must be added ϕ_{AD} and ϕ_{OC}, which affect greatly the viscosity of CWM. [B] in this figure is the case of material without water adsorption and occlusion. ϕ_I in this material corresponds to ϕ_0 of CWM and may be obtained on the basis of the case of glass in which ϕ_{OC} seems to be negligibly small, that is, $\phi_I=\phi_0$(glass)$+\phi_{AD}$(glass), being approximately 0.44.

ϕ_{OC} corresponds to $\phi_I-(\phi_0+\phi_{AD})$ and its dependency on coal rank is shown in **Fig. 9**. Although the results are rather scattered, it may be said that it reaches a constant level above about 85% carbon content. Here, ϕ_{AD} was obtained from the results in Fig. 8, because it is difficult to measure the mean value of ϕ_{AD} in CWM.

In the cases of higher-rank coals and glass which are difficult to coagulate, viscosity begins to increase steeply when the volume fraction increases to appreciably high levels, bringing about high ϕ_0 and α. On the contrary, in lower-rank coals, which have higher ϕ_{AD} and ϕ_{OC} and thus lower ϕ_0, α is relatively low except in the case of extremely low-rank coals below about 70% carbon content (Fig. 5). This is probably because of an increase in free water through rearrangement of coagulated particles and release of occluded water with the increase of shear force applied during viscosity measurement.

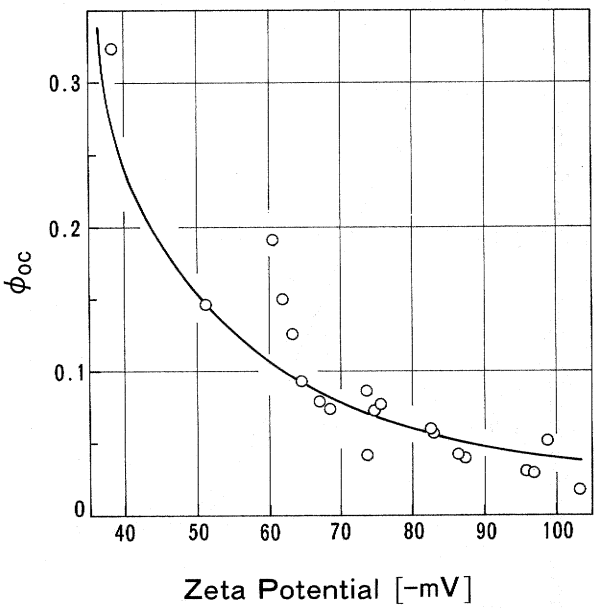

Fig. 11. Relation between zeta potential and ϕ_{OC} (Dispersant added in CWM: 0.5 wt%)

As revealed in Fig. 4, α of glass is very high and independent of particle size, showing that the viscosity is mainly due to friction between particles and is hardly affected by particle coagulation.

3.4 Viscosity characteristics and other properties

The relation between zeta potential and carbon content of coal is given in **Fig. 10**. C_0 point is also about 85% carbon.

The relation of ϕ_{OC} to zeta potential is revealed in **Fig. 11**, in which the curve is depicted so that ϕ_{OC} is

inversely proportional to the square of zeta potential, being in general agreement with the trend of experimental results. If it is possible to adopt zeta potential instead of surface potential of particles in the DLVO theory of the stability of dispersed particles, the repulsion force inhibiting coagulation of particles may be proportional to the square of zeta potential. Accordingly, it may be reasonable to assume as stated in the previous section that ϕ_{OC} may be regarded as measures of the degree of particle coagulation and the quantity of occluded water.

4. Conclusions

Viscosity characterizations were investigated using twenty kinds of coal from various countries and locations from the standpoint of rank of coal as bulk material to establish an evaluation system of coals for CWM.

(1) Various parameters of viscosity described in Fig. 2-b, such as ϕ_0, α and ϕ_{1000}, show a generally similar trend of reaching a constant level (**Fig. 12** Curve a) instead of continuing to change (Fig. 12 Line b) above about 85% carbon content of coal as the case of oxygen content (Fig. 1) or various physical properties as bulk material. The trend shown by Fig. 12 Curve a is an outstanding feature of the viscosity characteristics of CWM.

(2) Zeta potential, quantities of water adsorption on coal surface and of occuluded water within aggregates of coal particles exhibit a similar trend.

(3) Three types of flow can be seen in CWM, depending on coal rank. Those are P-I, Os and P-II.

(4) These results on various parameters are rather scattered, and it is presumed necessary to study coal not only as bulk material but also on the basis of surface chemistry.

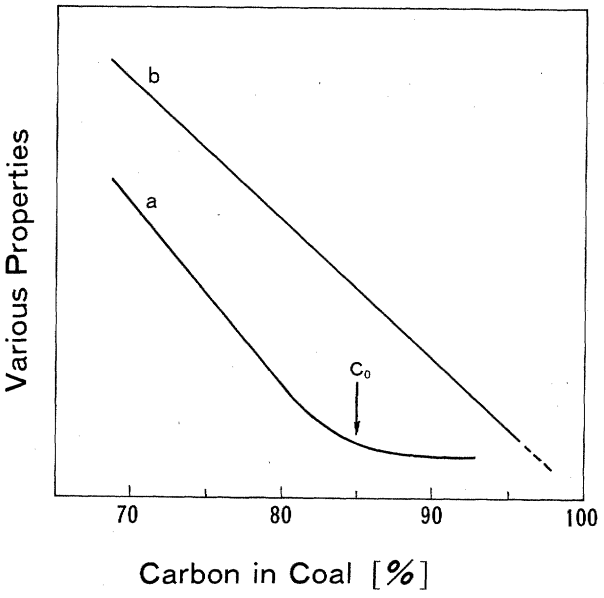

Fig. 12. Schematic representation of two types of carbon dependence in coal

Nomenclature

C_0	=	carbon content in coal when various parameters reach a constant level	[wt%]
D	=	mean particle size of coal powder	[μm]
α	=	slope of linear line in $\log\eta$[mPa·s]–ϕ plot	[—]
η	=	apparent viscosity of CWM	[mPa·s]
ϕ	=	volume fraction of coal powder in CWM, obtained from weight percent of coal in CWM on the basis of measurement of volume of coal powder per weight by helium substitution method	[—]
ϕ_0	=	volume fraction of coal powder in CWM, introduced by interpolating linear line in $\log\eta-\phi$ plot	[—]
ϕ_{1000}	=	volume fraction of coal powder in CWM at 1000 mPa·s	[—]
ϕ_{AD}	=	volume fraction of water adsorbed on coal surface in CWM	[—]
ϕ_I	=	volume fraction of particles without water adsorption and occlusion, being constant (=0.44)	[—]
ϕ_{OC}	=	volume fraction of water occluded within aggregates of particles	[—]
ϕ_R	=	volume fraction of restricted water in CWM	[—]

Literature Cited

1) Allendice, D. J. and D. G. Evans: *Fuel*, **50**, 231 (1971).
2) Brenner, D.: *Fuel*, **63**, 1324 (1984).
3) Chapman, R. N.: *US. DOE. Rep.*, SAND-1462C (1986).
4) Fuerstenau, D. W.: US. DOE. Rep., DOE-PC-70776-T-1-6 (1984).
5) Hatami, M., S. Ozawa and H. Sugimura: *J. Fuel Soc. Japan*, **46**, 819 (1967).
6) Honda, H., K. Ogino, M. Abe and S. Kawano: *J. Fuel Soc. Japan*, **65**, 341 (1986).
7) Kaji, R.: *J. Fuel Soc. Japan*, **65**, 847 (1986).
8) Mahajan, D. J.: *Powder Technol.*, **40**, 1 (1984).
9) Mahajan, D. J. and P. L. Walker, Jr.: *Fuel*, **50**, 308 (1974).
10) Matturo, M. G., R. Liotta and J. J. Isaacs: *J. Org. Chem.*, **50**, 5560 (1985).
11) Naka, A., Y. Nishida and T. Murata: *J. Fuel Soc. Japan*, **65**, 408 (1986).
12) Schafer, H. N. S.: *Fuel*, **49**, 197 (1970).
13) Stuart, A. D.: *Fuel*, **65**, 1003 (1986).